Scientific Research Publishing

Open Journal of Metal, 2022, 12, 1-9
https://www.scirp.org/journal/ojmetal
ISSN Online: 2164-277X
ISSN Print: 2164-2761

Rigorous Electromagnetic Modeling of a Micro Strip Line Incorporating a Flat and Thick Metallic Conductor Based on the Skin Effect Phenomenon

Rafika Mejri, Taoufik Aguili

Communication System Laboratory Sys'Com, National Engineering School of Tunis, University Tunis El Manar, Tunis, Tunisia
Email: mejrirafika@yahoo.fr, Taoufik.Aguili@gmail.com

How to cite this paper: Mejri, R. and Aguili, T. (2022) Rigorous Electromagnetic Modeling of a Micro Strip Line Incorporating a Flat and Thick Metallic Conductor Based on the Skin Effect Phenomenon. *Open Journal of Metal*, **12**, 1-9.
https://doi.org/10.4236/ojmetal.2022.121001

Received: January 13, 2022
Accepted: March 27, 2022
Published: March 30, 2022

Abstract

In most studies of microstrip circuits, the majority of researchers assume that the microstrip structures studied have flat metallic conductors of finite widths but without thickness. But in reality these types of structures integrate metallic copper conductors of different thicknesses. If we neglect this thickness we introduce error in the electrical parameters of the microstrip structure, which affects the effective permittivity, the characteristic impedance, the adaptation of the circuit, the resonance frequency, etc. Given the importance of this parameter (thickness of the metal of micro rubon structures), rigorous electromagnetic modeling of the thick micro rubon line based on the skin effect phenomenon (In fact at high frequency the skin effect phenomenon occurs and the current only flows on the periphery of the conductor) has been proposed to improve the studied electric model and ensure the increase in the precision of the analysis method used: Wave concept iterative process. The good agreement between the simulated and published data justifies the improvement of the model.

Keywords

Micro Strip Line, Thick Conductor, WCIP, Skin Effect Phenomenon

1. Introduction

The iterative method is based on the concept of waves for the study of simple or multilayer planar structures and arbitrary shapes. The advantage of this method is its great ease of implementation and speed of execution mainly due to the systematic use of a fast Fourier transform in modes. So the behavior of a single or

multilayer structure can be summarized by boundary conditions expressed at the global interface [1] [2] [3] [4]. These methods need to be improved and require updates as the evolution of these circuits is very fast. The manufacture of new circuits, non-stop and progressive, forces researchers to adapt their simulation tools, which requires the development of the numerical methods characterizing these devices.

The new formulation of the wave concept iterative method (FWCIP) [5] [6] [7] [8] extends it to the study of planar structure integrating flat and thick conductors. This method is based on the concept of waves for solving the problems of electromagnetic diffraction. Its principle is similar to that used in the TLM method (spatial mesh differential method). In this study, the circuit to be studied is placed in a case with metal walls. It makes it possible to define a basis for the decomposition of the electromagnetic field.

Model 1 Figure 1 proposed in this article, takes into account all faces of the metal conductor. Unlike model 2 Figure 2 was studied previously [9] [10].

2. Theory

Study Structure

Figure 3 shows the new electromagnetic model of the study structure. It consists of three layers of different materials. The first layer is filled with a dielectric material of relative permittivity ε_{r1} and thickness h_1. It lies between the ground

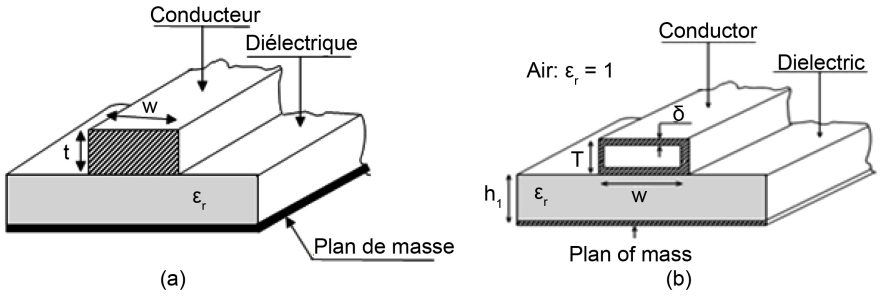

Figure 1. Study structure (Model 1). (a) Real structure. (b) Structure based on the skin effect phenomenon.

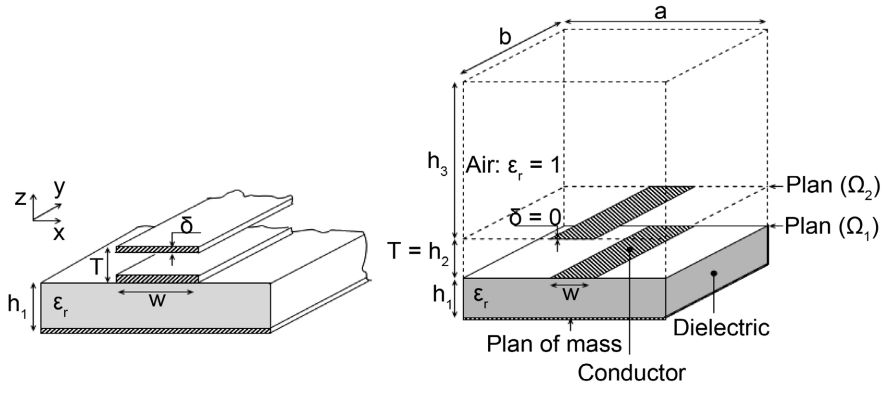

Figure 2. Study structure (Model 2).

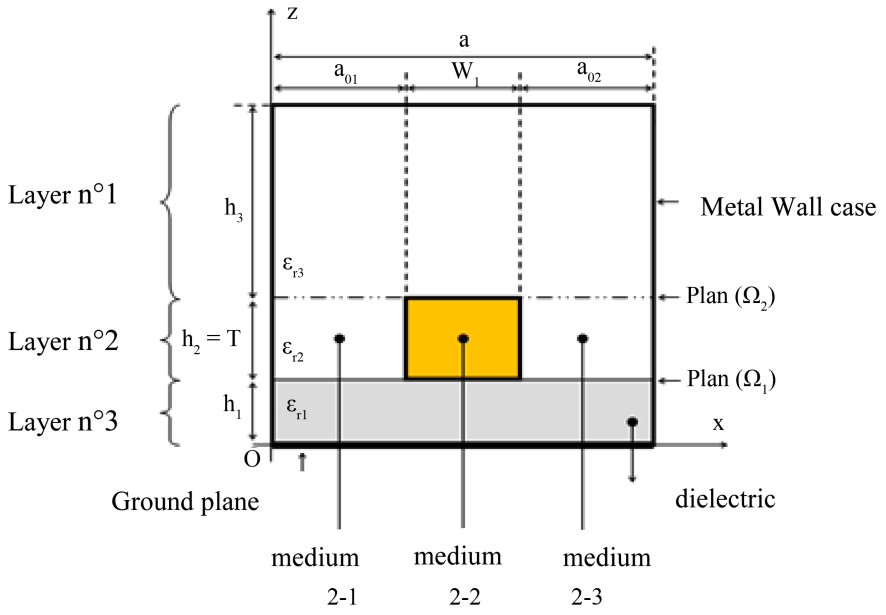

Figure 3. Study structure (Model 1).

plane of the study structure and the discontinuity plane Ω_1. The second layer is placed between the two planes of discontinuities Ω_1 and Ω_2. It consists of three environments. Medium 2-1 is a rectangular waveguide with metal walls. It is filled with air and of dimensions "$a_{01} \times b \times h_2$". The medium 2-2 is occupied by the metal conductor of dimensions "$w_1 \times L \times h_2$". Inside this region the E_{int} field and the J_{int} current are void. According to the principle of the skin effect, microwave current circulates only on the periphery of the conductor. Medium 2-3 is a rectangular waveguide with metal walls. It is filled with air and of dimensions "$a_{02} \times b \times h_2$". Layer 3 is filled with air. It is located between the discontinuity plane Ω_2 and the top cover of the metal housing that surrounds the entire study structure.

Between the metal conductor (medium 2-2) and the walls of the housing are formed the two rectangular waveguides occupying the media (2-1 and 2-3). They are therefore made up of the three electric walls of the housing and one of the faces of the metal conductor parallel to the Oyz plane. The passage of waves from plane Ω_1 to plane Ω_2 Figure 4 (or from plane Ω_2 to plane Ω_1) is done through these two waveguides. The medium 2-2 occupied by the metal conductor will not be crossed by any waves (incident and reflected).

Study structure parameters Figure 5: a = 18.4 mm, b = 24 mm, c_1 = 0.75 mm, d_1 = 0.375 mm, w_1 = 2.3 mm, h_1 = 1.52 mm, h_2 = 10 µm, h_3 = 14.99 mm, ε_{r1} = 4.32, ε_{r2} = 1, ε_{r3} = 1.

The diagram in Figure 6 summarizes the evolution of the multilayer iterative method, introducing into the calculations the effect of the two faces, from the metal conductor parallel to the Oyz plane. The Q_1 and Q_2 quadrupoles model these two waveguides that channel incident and reflected waves from layer 1 to layer 3.

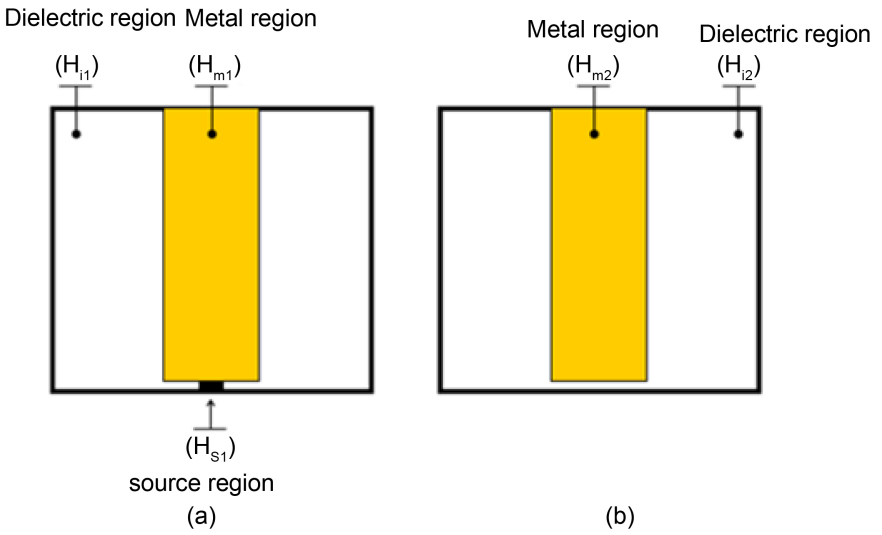

Figure 4. Definition of the different regions of the planes of discontinuities. (a): Plane Ω_1. (b): Plane Ω_2.

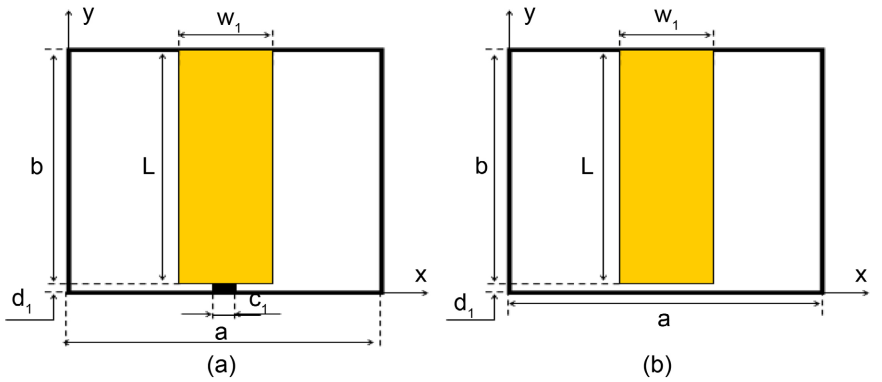

Figure 5. Citations of the planes' discontinuities. (a): Plane Ω_1. (b): Plane Ω_2.

$\hat{\Gamma}_{\Omega 1}$ et $\hat{\Gamma}_{\Omega 2}$: Diffraction operators, giving the incident waves from the reflected waves that diffract at the level of the planes of discontinuities (Ω_1 et Ω_2). They are defined in the space domain.

$\hat{\Gamma}_k$: Reflection operator ensuring the link between incident waves and reflected waves. It is defined in the spectral range $k \in$ {medium 1, medium 3}.

α: Te (Transverse Electrical), TM (Transverse Magnetic) mode indicator;

n: Number of iterations.

$\hat{\Gamma}_{Qi}$: Reflection operator defined in the spectral domain. We find in this operator the nature of the walls which enclose the media 2-1 and 2-3, of layer n˚2 (**Figure 4**). We also find in this operator the nature of the dielectric filling these two medias. This operator connects the incident waves "$\vec{A}_{21}$, $\vec{A}_{22}$" reflected waves "$\vec{B}_{21}$, $\vec{B}_{22}$" when they move from the spatial domain to the spectral domain.

The expressions below relate the incident waves "$\vec{A}_1$, $\vec{A}_{21}$, $\vec{A}_{22}$ et $\vec{A}_3$" reflected waves "$\vec{B}_1$, $\vec{B}_{21}$, $\vec{B}_{22}$ and $\vec{B}_3$" when they pass from the spatial domain to the spectral domain.

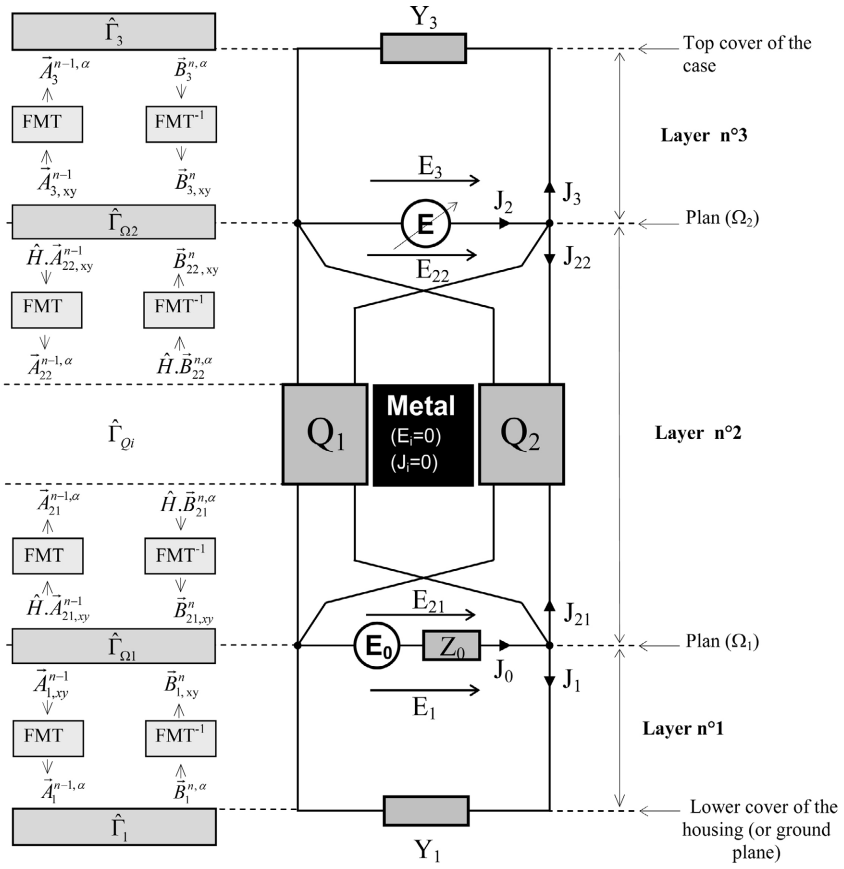

Figure 6. Electrical diagram modeling the study structure.

$$\begin{pmatrix} A_1 \\ A_{21} \end{pmatrix} = \hat{\Gamma}_{\Omega 1} \begin{pmatrix} B_1 \\ B_{21} \end{pmatrix} + \begin{pmatrix} A_1^0 \\ A_2^0 \end{pmatrix}$$

$$\begin{pmatrix} B_{21} \\ B_{22} \end{pmatrix} = \hat{\Gamma}_{Qi} \begin{pmatrix} A_{21} \\ A_{22} \end{pmatrix}$$

$$\begin{pmatrix} A_{22} \\ A_3 \end{pmatrix} = \hat{\Gamma}_{\Omega 2} \begin{pmatrix} B_{22} \\ B_3 \end{pmatrix}$$

$$\begin{pmatrix} \vec{J}_{21} \\ \vec{J}_{22} \end{pmatrix} = \begin{pmatrix} \hat{Y}_{11} & \hat{Y}_{12} \\ \hat{Y}_{21} & \hat{Y}_{22} \end{pmatrix} \begin{pmatrix} \vec{E}_{21} \\ \vec{E}_{22} \end{pmatrix}$$

According to the diagram of Figure 6, we can write:

$$\begin{cases} \vec{J}_0 = \vec{J}_1 + \vec{J}_{21} \\ \vec{J}_2 = \vec{J}_{22} + \vec{J}_3 \\ \vec{J}_1 = \hat{Y}_1 \cdot \vec{E}_1 \\ \vec{J}_3 = \hat{Y}_3 \cdot \vec{E}_3 \\ \vec{E}_1 = \vec{E}_{21} \\ \vec{E}_{22} = \vec{E}_3 \end{cases}$$

FMT (Modal Fourier Transform) is a function for defining the amplitudes of the TE (Transverse Electrical) and TM (Transverse Magnetic) modes in the

spectral domain. Its use in the iterative method significantly reduces computational time and accelerates the passage of incident waves from the spatial domain to the modal domain) [11] [12]:

$$\begin{bmatrix} \left[A_k^{TE}\right] \\ \left[A_k^{TM}\right] \end{bmatrix} = \mathrm{FMT} \begin{bmatrix} \left[A_{k,x}\right] \\ \left[A_{k,y}\right] \end{bmatrix}$$

And also accelerates the passage of reflected waves from the modal domain to the spatial domain:

$$\begin{bmatrix} \left[B_{k,x}\right] \\ \left[B_{k,y}\right] \end{bmatrix} = \mathrm{FMT}^{-1} \begin{bmatrix} \left[B_k^{TE}\right] \\ \left[B_k^{TM}\right] \end{bmatrix}$$

The (FMT) and (FMT^{-1}) symbolize respectively the direct and inverse Fourier transform in modes.

FMT requires the discretization of the spatial and modal domains. The discretization of the first domain is achieved by meshing the different regions of the planes Ω_1 and Ω_2 into small "pixel" surfaces whose dimensions are linked to the dimensions of the passive components included in the considered plane. In this domain, the interaction between pixels is not considered in the formulation of the method. On the other hand, the use of the FMT introduces implicit pixel coupling in the modal domain. The electromagnetic quantities and the waves (incident and reflected) are represented by matrices whose dimensions depend on the density of the mesh chosen in the spatial domain.

Part of layer 2 of the study structure is filled with air (media 2-1 and 2-3) the other part is occupied by the metallic conductor (medium 2-2). To separate these two domains we use the operator $\hat{H}$ which is a Heaviside echelon defined below. The operators $\hat{H}_i$, $\hat{H}_S$ are defined as follows:

$$\hat{H}_i = \begin{cases} 1 & \text{on the dielectric region} \\ 0 & \text{elsewhere} \end{cases}$$

$$\hat{H}_S = \begin{cases} 1 & \text{on the excitation source region} \\ 0 & \text{elsewhere} \end{cases}$$

We can write the operator $\hat{H}$ depending on the operators $\hat{H}_i$ et $\hat{H}_S$:

$$\hat{H} = \hat{H}_i + \hat{H}_S = \begin{cases} 1: & \text{in the medium filled with air} \\ 0: & \text{in the medium occupied by the metallic conductor} \end{cases}$$

3. Validation of Simulation Results

Figure 7 shows the variation of the resonance frequency, the input impedance of the study structure, as a function of the thickness of the metal used. We find in this figure a comparison between the results of the two models, model 1 and model 2, with those calculated by Ansoft's HFSS software. If the thickness of the metal used increases, the results of the model in Figure 1 get closer to the results calculated by Ansoft's HFSS software. These results show that the model in Figure 1 is more rigorous. This model ensures an increase in the accuracy of the

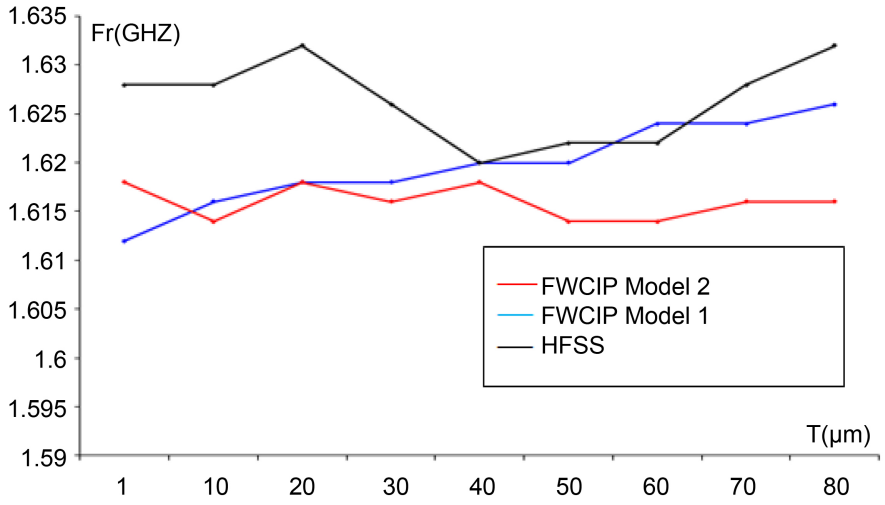

Figure 7. Variation of the resonance frequency of the input impedance of the study structure according to the thickness of the metal used.

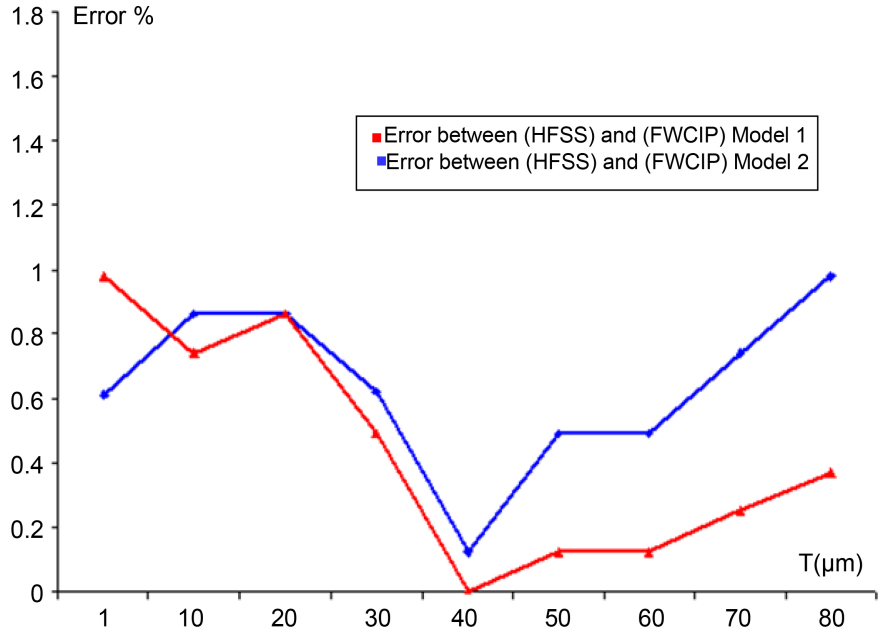

Figure 8. Variation in relative error on the resonance frequency of Ze depending on the thickness of the metal used.

analytical method used.

Figure 8 shows the relative error on the resonance frequency of the input impedance of the study structure. This depends on the thickness of the metal used. This figure shows a comparison of the relative error between the results calculated by Ansoft's HFSS software and those calculated by the iterative method (models in Figure 1 and Figure 2). We note that the model 1 has a smaller error than the model 2. This is for a flat metal conductor whose thickness varies from 10 μm to 80 μm. These results confirm that the model in Figure 1 increases the accuracy of the analytical method used.

4. Conclusion

In this article we have shown the effectiveness of the correction made to the iterative method by the model 1 we have proposed. The latter ensures the modeling of planar structures integrating flat metal conductors with a significant thickness. The results found are compared with those calculated by Ansoft's HFSS software showing the improvement made to the iterative method FWCIP.

Conflicts of Interest

The authors declare no conflicts of interest regarding the publication of this paper.

References

[1] Serres, A., Serres, G.K.F., Fontgalland, G., Freire, R.C.S. and Baudrand, H. (2014) Analysis of Multilayer Amplifier Structure by an Efficient Iterative Technique. *IEEET Transaction on Magnetics*, **50**, 185-188. https://doi.org/10.1109/TMAG.2013.2285601

[2] Jan, J.-Y., Pan, C.-Y., Chang, F.-P., Wu, G.-J. and Huang, C.-Y. (2012) Realization of Compactand Broadband Performances Using the Microstrip-Line-Fed Slot Antenna. *Proceedings of APMC* 2012, Kaohsiung, 4-7 December 2012, 1379-1381. https://doi.org/10.1109/APMC.2012.6421925

[3] Kosslowski, S. (1988) The Application of the Point Matching Method to the Analysis of Microstrip Lines with Finite Metallization Thickness. *IEEET Ransactions on Microwave Theory and Techniques*, **36**, 1265-1271. https://doi.org/10.1109/22.3668

[4] Feng, N.N., Fang, D.D. and Huang, W.P. (1998) An Approximate Analysis of Microstrip Lines with Finite Metallization Thickness and Conductivity by Method of Lines. *Proceedings of the International Conference on Microwaveand Millimeter Wave Technology*, Beijing, 18-20 August, 1053-1056. https://doi.org/10.1109/ICMMT.1998.768471

[5] Farina, M., *et al.* (2000) Spectral Domain Approach to 2D-Modelling of Open Planar Structures with Thick Lossy Conductors. *IEE Proceedings—Microwaves, Antennas and Propagation*, **147**, 321. https://doi.org/10.1049/ip-map:20000732

[6] Shih, C. (1989) Frequency-Dependent Characteristics of Open Microstrip Lines with Finite Strip Thickness. *IEEE Transactions on Microwave Theory and Techniques*, **37**, 793-795. https://doi.org/10.1109/22.18856

[7] Henri, B., Sidima, W. and Damirnne, B. (2002) The Concept of Waves: Theory and Applications in Electronic Problems. *Proceeding of the* IX*th International Conferenceon Mathematical Methodsin Electromagnetic Theory*, Kiev, Ukraine, 10-13 September, 100-104. https://doi.org/10.1109/MMET.2002.1106841

[8] Serres, A., Fontgalland, G., de Farias, J.E.P. and Baudrand, H. (2010) An Efficient Algorithm for Planar Circuits Design. *IEEE Transactions on Magnetics*, **46**, 3441-3444. https://doi.org/10.1109/TMAG.2010.2044150

[9] Mejri, R. and Aguili, T. (2016) A New Approach Based on Iterative Method for the Characterization of a Micro-Strip Line with Thick Copper Conductor. *Journal of Electromagnetic Analysis and Applications*, **8**, 95-108. https://doi.org/10.4236/jemaa.2016.85010

[10] Mejri, R. and Aguili, T. (2016) New Formulation of the Multilayer Iterative Method:

Application to a Coplanar Lines with Thick Conductor. J*ournal of Electromagnetic Analysis and Applications*, **8**, 197-218. https://doi.org/10.4236/jemaa.2016.89019

[11] Kaddour, M., Mami, A., Gharsallah, A., Gharbi, A. and Baudrand, H. (2003) Analysis of Multilayer Microstrip Antennas by Using Iterative Method. *Journal of Microwaves and Optoelectronics*, **3**, 39-52.

[12] Lamhene, Y., Tellache, M., Haraoubia, B. and Baudrand, H. (2009) Triangular Discretization for Analysis of Microstrip Mitred Bend, by an Iterative Method Using the Fast Modal Transform. *International Journal of Computing*, **8**, 33-40. https://doi.org/10.47839/ijc.8.2.664